Chemical Engineering Journal 433 (2022) 133520

Contents lists available at ScienceDirect

Chemical Engineering Journal

journal homepage: www.elsevier.com/locate/cej

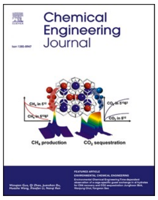

Bis(3-(trinitromethyl)-1H-1,2,4-triazol-5-yl)methanone: A mildly acidic high-performing energetic material

Ajay Kumar Chinnam [a], Jatinder Singh [a], Richard J. Staples [b], Jean'ne M. Shreeve [a,*]

[a] Department of Chemistry, University of Idaho, Moscow, ID 83844-2343, USA
[b] Department of Chemistry, Michigan State University, East Lansing, MI 48824, USA

ABSTRACT

High performance, acceptable thermostability, and low mechanical sensitivity are high-demand properties in the design of competitive materials. Nitrogen-rich compounds are an alternative source of green molecules. Two simple, efficient synthetic routes to a novel material, bis (3-(trinitromethyl) – 1H-1,2,4-triazol-5-yl) methanone, **5**, by using inexpensive starting compounds are described. Compound **5** has interesting chemical reactivity with water in the presence of organic solvents to form a *gem* diol of bis (3-(trinitromethyl) – 1H-1,2,4-triazol-5-yl) methanediol, **5a**. All new molecules are well characterized by advanced spectroscopic techniques. The structures of **5**·Et_2O, **5a**·$3H_2O$, and salt **6** are confirmed by single-crystal X-ray analysis. The densities of the solid powder compound **5**, and the crystals of **5a**·$3H_2O$ were measured by a gas pycnometer. The theoretical densities and Explo5 calculations of solvent-free molecules, **5** and **5a,** suggest that expanding the functionality of carbonyl-bridged compounds may be an alternative way to achieve high-performing materials.

1. Introduction

Research and development of High energy density materials (HEDMs) have made significant advances in the past few decades. Their wide variety of uses are found in the fields of civil engineering and space exploration.[1,2] However, there are few such powerful chemical materials and benchmarks for current HEDMs, such as 1,3,5-trinitroperhydro-1,3,5-triazine (RDX) and 1,3,5,7-tetranitro-1,3,5,7-tetrazoctane (HMX).[3] They share some degree of structural similarity at the molecular level which gives rise to high mechanical sensitivity and they often release undesirable residues into the atmosphere.[4] Therefore, current research is focused on the development of novel materials based on nitrogen-rich compounds possessing high density, high thermostability, and better mechanical sensitivity.[5] A large number of energetic N—N and C—N bonds in their structures enhance the high heat of formation and high density, which results in the overall performance of the nitrogen-rich parent skeleton.[6] As a result, five-membered ring heterocycles (pentazole, tetrazole, triazole, pyrazole, furazan, etc.) are found to be promising building blocks for such new materials.[7] The nitrogen-rich 1,2,4-triazole ring is frequently encountered as a key heterocyclic system in several worthwhile materials because of having a high heat of formation and thermal stability, and the carbon atoms at the 3 and 5 positions are accessible for attaching high performing groups.[8] Explosphores, such as nitro, nitroamino, dinitromethyl, and trinitromethyl groups, are very useful in improving the density and oxygen balance, which proportionally increase the detonation properties of the resultant materials.[9–12] Several synthetic strategies have been utilized for the mono, bis, or fused triazole-based materials with the combination of nitro, dinitromethyl, and trinitromethyl groups.[13–16] In this category, high density, and positive oxygen balance were achieved by 1H-1,2,4-triazoles, compound **A** [17] (1.94 g cm^{-3}; +9.12 %), while the other two bistriazole compounds have lower densities and oxygen balances, **B** [18,19] (1.89 g cm^{-3}; −3.69 %), and **C**[17] (1.83 g cm^{-3}; −8.60 %) (Fig. 1). The thermal decomposition of **A** (124 °C) is lower than that of **B** and **C**, while they have a higher thermostability of 133 °C.

Compound **C** is very sensitive to impact (1.5 J), which results in it being very difficult to handle or to store for practical use. Recently, our group reported the poly trinitromethyl bis-triazole derivative **D**, with improved thermostability and impact sensitivity obtained by introducing a carbonyl group between the two polynitrotriazoles, giving high density and positive oxygen balance (1.94 g cm^{-3}; +8.70 %). Compound **D** was found to behave as a highly dense green oxidizer, while it has lower detonation properties due to the presence of *N*-trinitromethyl groups.[20] Therefore, we were encouraged to utilize this methodology for designing new triazoles with *C*-trinitromethyl groups, which could have superior thermostability, and detonation properties such as bis *C*-trinitromethyl triazoles with a carbonyl bridge, viz., bis(3-(trinitromethyl)-1H-1,2,4-triazol-5-yl)methanone, **5** (Fig. 1).

Very interestingly compound **5** was found to react with a molecule of

---

* Corresponding author.
E-mail address: jshreeve@uidaho.edu (J.M. Shreeve).

https://doi.org/10.1016/j.cej.2021.133520
Received 30 August 2021; Received in revised form 11 October 2021; Accepted 5 November 2021

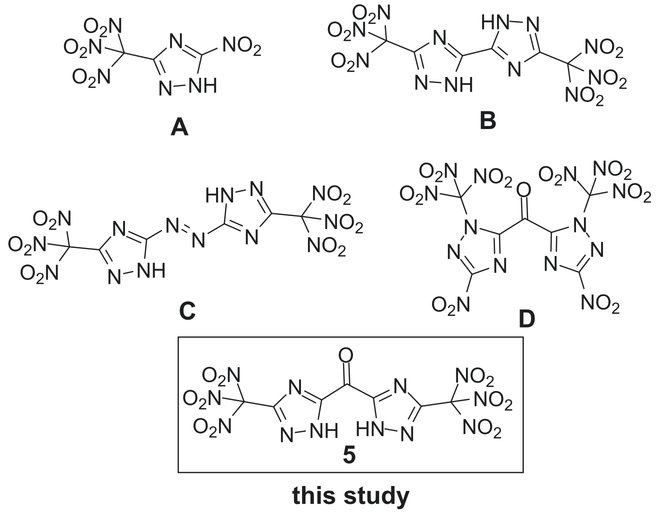

Fig. 1. Selected 1,2,4-triazoles of polynitromethyl and target molecule in this study.

water in the presence of an organic solvent to form *a gem* diol derivative of **5a**. This is the result of the presence of the carbonyl group between two highly electron-deficient 1,2,4-triazoles.[21] Similar behavior in carbonyl bridged bis tetrazoles was observed recently, during the oxidation of di(1H-tetrazol-5-yl)methane.[22,23] To our knowledge, the *gem* diol is unstable or does not exist, when exposed to acid or heat since it will be redirected to the carbonyl form. The carbonyl-*gem* diol equilibrium can be of vital importance in the field of biochemistry [24] but so far no such compounds were reported in the field of high density materials. All new compounds were fully characterized by NMR, FTIR, elemental analysis, and Differential scanning calorimetry (DSC). Structures of **5**·Et_2O, **5a**·$3H_2O$, and **6** were characterized by single crystal X-ray crystallography. In addition to its reactivity with a water molecule in the presence of organic solvents, **5** has detonation properties superior to RDX and comparable to HMX.

2. Results and discussion

2.1. Synthesis

As shown in Scheme 1, the initial precursor, diethyl 2,2′-(methylenebis(1H-1,2,4-triazole-5,3-diyl))diacetate, **3**, was obtained by refluxing a mixture of malonohydrazide, **1**, and ethyl 3-ethoxy-3-iminopropanoate **2** (1:2 ratio) in ethanol. Later, **3** was hydrolyzed using 10 M sodium hydroxide followed by acidification to give **4**. Then compound **4** was nitrated in the presence of sulfuric and nitric acids at 0–5 °C (Method A). After 24 h, the reaction mixture was poured into ice-cold water, and a colorless precipitate was collected by filtration and dried at room temperature to give compound **5** in 86.6% yield. Another approach was used for the synthesis of **5**. The diester derivative, **3** was nitrated and neutralized with aqueous ammonia to give the diammonium salt, **6**. Further nitration of **6** in mixed acid gave a product that was isolated by pouring the reaction mixture into ice-cold water, followed by filtration and drying at room temperature giving a colorless solid **5** in 72% yield (Method B). Isolation of product **5** from ice-cold water shows that it is stable in water.

2.2. Spectroscopy

All the new compounds were fully characterized by FTIR and NMR (^{1}H and ^{13}C) spectroscopy, and elemental analysis (SI). As discussed in the Introduction and shown in Fig. 2, compound **5** was found to give different NMR spectra in two different NMR solvents. Deuterated solvents, d_6-DMSO and d_3-MeCN, were purchased from Cambridge Isotope Laboratories, Inc., and the NMR spectra were measured at 25 °C. Details of NMR experimental studies are included in the SI. The ^{13}C NMR spectrum of compound **5** offers evidence that the compound exists with the carbonyl (**5**) or *gem* diol bridge (**5a**) between the two triazole rings. In d_6-DMSO, the ^{13}C NMR of **5**, four signals are seen with the signal at 88.7 ppm assigned to the *gem* diol carbon (Fig. 2, top), while the signal at 166.9 ppm (in d_3-MeCN) is the carbonyl carbon (Fig. 2, below). The NMR results were identical for compound **5** which was prepared from Method **A** and **B**. Since we have isolated compound **5** from water as an insoluble white solid and confirmed by ^{13}C NMR in d_3-MeCN and combustion elemental analysis, it is likely that it is stable in pure water but not in organic solvents which absorb water because the two adjacent highly electron-deficient 1,2,4-triazoles which are mildly acidic may catalyze the carbonyl to hydrolyze in organic solvents (Scheme 2).[21]

^{15}N NMR Spectra. The ^{15}N NMR spectra of **5a**, and **6** were determined in d_6-DMSO (Fig. 3). In the spectrum of **5a** four signals are seen for the nitrogen atoms of trinitromethane at $\delta = -32.3$ (N1), and the triazole ring nitrogen signals at $\delta = -75.0$, (N2), $\delta = -126.1$ (N3) and $\delta = -157.0$ (N4). In the spectrum of **6**, the nitrogen signal for the ammonium cation is shifted to higher field ($\delta = -360.1$ ppm (N5)) and the nitrogen signal for dinitromethane is shifted to lower field at $\delta = -22.0$ (N1). The triazole ring nitrogen signals are at $\delta = -75.8$ (N2), $\delta =$

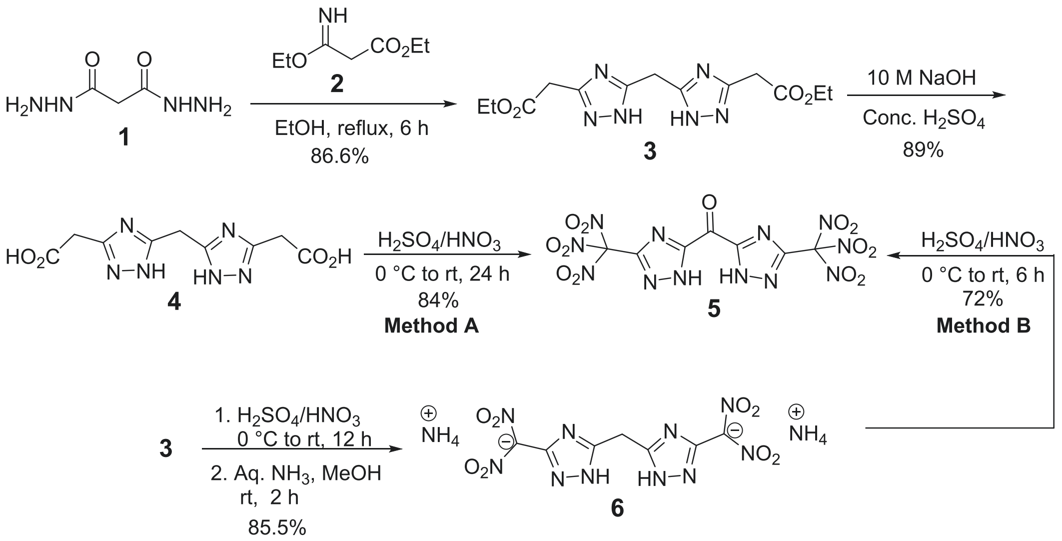

Scheme 1. Synthesis of bis(3-(trinitromethyl)-1H-1,2,4-triazol-5-yl)methanone, **5**.

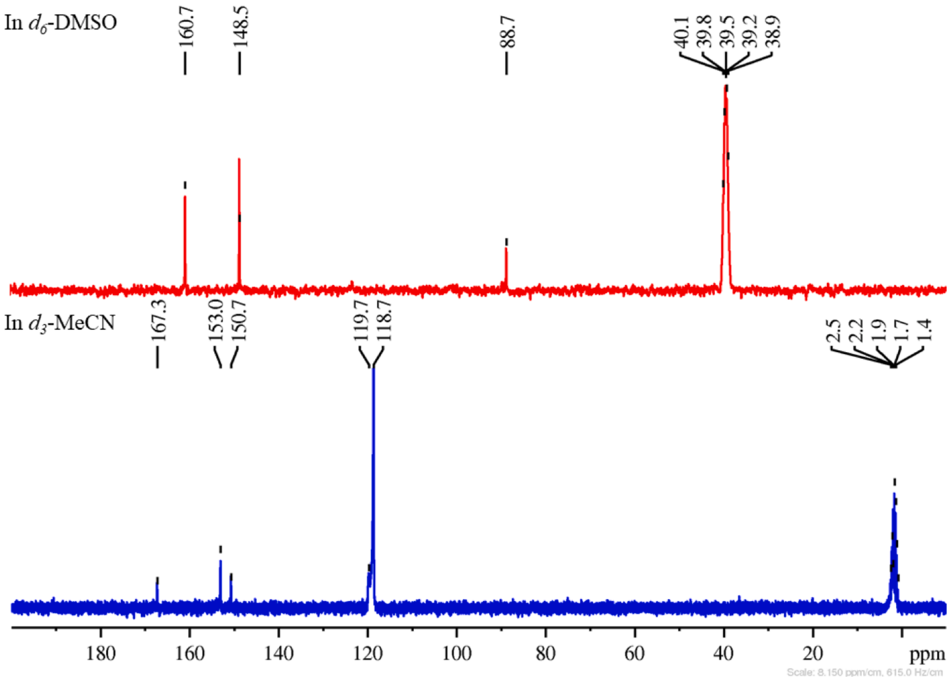

Fig. 2. ^{13}C NMR spectra of **5** in d_6-DMSO (top) and d_3-MeCN (below).

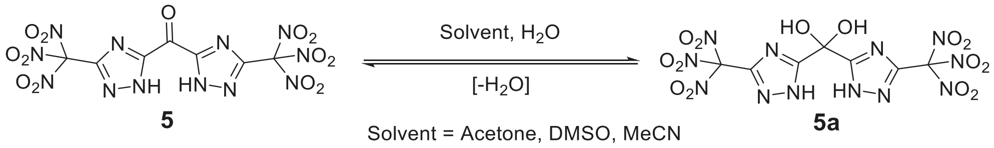

Scheme 2. Formation of *gem* diol **5a**.

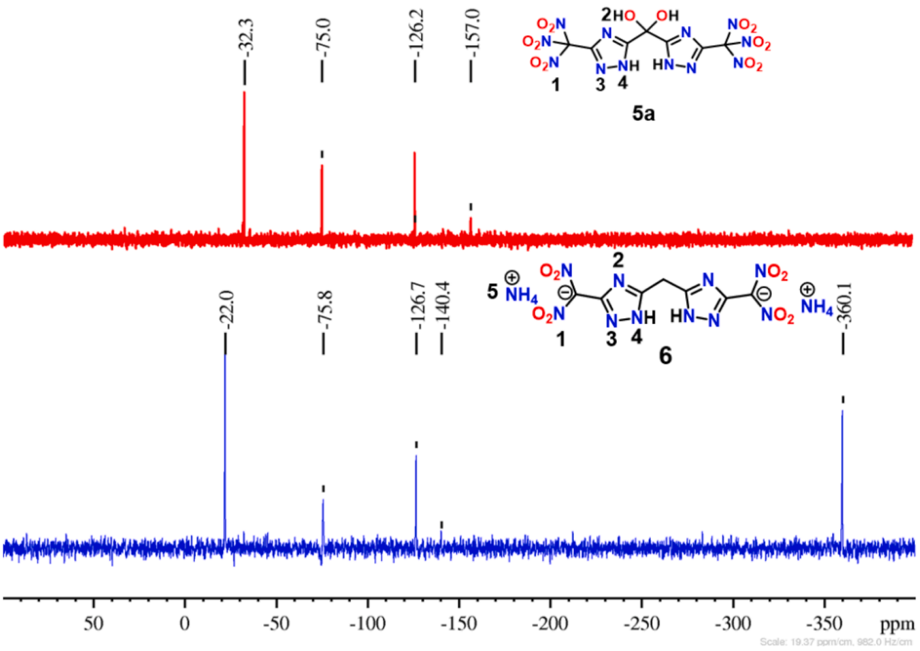

Fig. 3. ^{15}N NMR spectrum of **5a** and **6** in d_6-DMSO.

−126.7 (N3) and $\delta = -140.4$ (N4).

2.3. X-ray crystallography

Several methods were tried in order to obtain a crystal of compound **5** free of solvent but unfortunately, it was not possible. Because of the strong electrophilicity of the carbonyl group in **5**, it participated in H-bonding with solvents that were used for the crystallization leading to structures with solvent molecules or to conversion of the carbonyl to a *gem* diol with accompanying water molecules. To understand the structures of the carbonyl group in **5** and *gem* diol in **5a**, both structures were characterized by X-ray analysis. Suitable crystals of **5** and **5a** were obtained in ethyl acetate by allowing diethyl ether to diffuse into the solution and slow evaporation from a mixture of acetone and water, respectively. There is one Et_2O molecule per one molecule of **5** (in **5**·Et_2O) and three water molecules per two molecules of **5a** (in **5a**·$3H_2O$) in the crystal structures which are omitted for clarity (Figs. 4 and 5). Because of the solvent or water molecules, both the crystals have some structural disorder. All of them are well refined, and the details are in the SI. Compound **5**·Et_2O crystallized in the monoclinic space group $P2_1/c$ (Fig. 3a). Because of the presence of one ether molecule, the crystal density is quite low at 1.669 g cm^{-3} at 100 K. The bond lengths in the two triazole rings are between typical single and double bonds (SI). The C(1)=O(1) bond length is 1.207 (7) Å in **5**·Et_2O, which is considerably shorter than the standard C=O bond length from CSD at 1.24 Å for all C = O. It is 1.22 Å when between aromatic groups. The geometry around the bridging carbonyl carbon deviates slightly from trigonal planar with an angle of C(2)–C(1)–C(5) = 117.33(4)°. The dihedral angle between the mean planes through the two triazole rings is 20.62°. The trinitromethane moieties are nearly perpendicular to the triazole plane with the dihedral angle between the mean plane through the triazole rings and the mean plane through three nitrogen atoms of the $C(NO_2)_3$ groups found in the range of 85.28 to 87.83°. All atoms in the two triazole rings are nearly planar with the bridged carbonyl carbon having the torsion angles of N(3)–N(2)–C(2)–C(1) = 178.6 (5)° and N(9)–N(9)–C(5)–C(1) = 176.8 (4)°. The N—O bond distance of the NO_2 groups and the C—N bond distance of trinitromethane are typically between 1.174 and 1.222 Å and 1.509–1.546 Å, respectively. Bonds C3 − C4 and C6 − C7 are 1.493(7) and 1.509(8) Å, respectively. Also, in the crystal packing of **5**·Et_2O, an intramolecular hydrogen bond N(2) − H(2)···N(7) and two intermolecular hydrogen bonds, one with an adjacent molecule of **5**, N(2) − H(2)···N(1)# and another one with co-solvent of ether, N(8) − H(8)···O(14) (symmetry code: +x, ½-y, ½+z) form a three dimensional network (Fig. 4b).

Compound **5a**·$3H_2O$ crystallized in the monoclinic space group $C2/c$ with a calculated density of 1.849 g cm^{-3} at 100 K (Fig. 5a). The two triazoles in **5a**·$3H_2O$ are non-planar with the bridged carbon because it connected with *gem* diol. The *gem* diol and the attached carbon are nearly tetrahedral with two triazole ring carbons at an angle of C(2)–C(1)–C(5) = 107.87 (10)°. The *gem* diol moiety in the crystals of **5a**·$3H_2O$ is little impacted by thermal decomposition except by loss of water at 80 °C and a concomitant but a slight increase in impact sensitivity 11 J. Since it is a *gem* diol, the molecular structure is nonplanar, which may be the reason for the increase in the impact sensitivity of **5a**·$3H_2O$. The dihedral angles between the mean planes through the two triazole rings are 80.66°. In both triazole rings, all atoms are planar with torsion angles of C(2)-N(3)-C(3)-N(2) and C(5)-N(9)-C(8)-N(8) at −1.17° (14) and −0.93° (14), respectively. In the crystal packing of **5a**·$3H_2O$, there are three intermolecular hydrogen bonds between *gem* diol molecules **5a** and three water moleculaes N(1) − H(1)···O(1 W), N(7) − H(7)···O(2 W), and O(3 W) − H(3WB)···N(8) (Fig. 5b).

Compound **6** crystallizes in an orthorhombic space group $Pca2_1$ with four moieties in the unit cell and a crystal density of 1.801 g cm^{-3} at 100 K (Fig. 6). In crystal structure **6**, one NH_4 group and one NO_2 group have a disorder which was removed for clarity. The geometry of the bridging methylene carbon is nearly tetrahedral with two triazole ring carbons at an angle of C(2)–C(1)–C(7) = 108.8 (2)°. The dihedral angles between the mean planes through the two triazole rings are 88.87°. The packing diagram of **6** shows many strong intermolecular hydrogen bond interactions due to the presence of the ammonium cation, triazole NH, and nitro oxygen atoms (Fig. 6b).

2.4. Hirshfeld surfaces and fingerprint analysis

Since the physical properties of poly nitro compounds are strongly influenced by crystal packing, two-dimensional (2D) fingerprints and the associated Hirshfeld surfaces [25,26] were employed by using Crystalexplorer17.5 to understand intermolecular interactions in **5**·Et_2O and **5a**·$3H_2O$ (Fig. 7). As shown in Fig. 7a and 7b, red and blue dots on the Hirshfeld surface analysis represent high and low close contact, respectively. Red dots indicate intermolecular strong (N···O and O···N) interactions. In Fig. 7c and 7d, because of the carbonyl bridge and ether molecule or *gem* diol and three water molecules, the remarkable spikes on the bottom demonstrate strong O···H and N···H hydrogen bond (HB) interactions which contribute to the total weak interactions of 35.8% (**5**·Et_2O) and 36.5%(**5a**·$3H_2O$), respectively. Because of the high content of oxygen, there is a high percentage of interaction between oxygen and other elements. As shown in Fig. 7e, there are 16.1% N···O and 34.2% O···O interactions for **5**·Et_2O and 15.8% N···O and 37.3% O···O interactions for **5a**·$3H_2O$, which support the high crystal density and

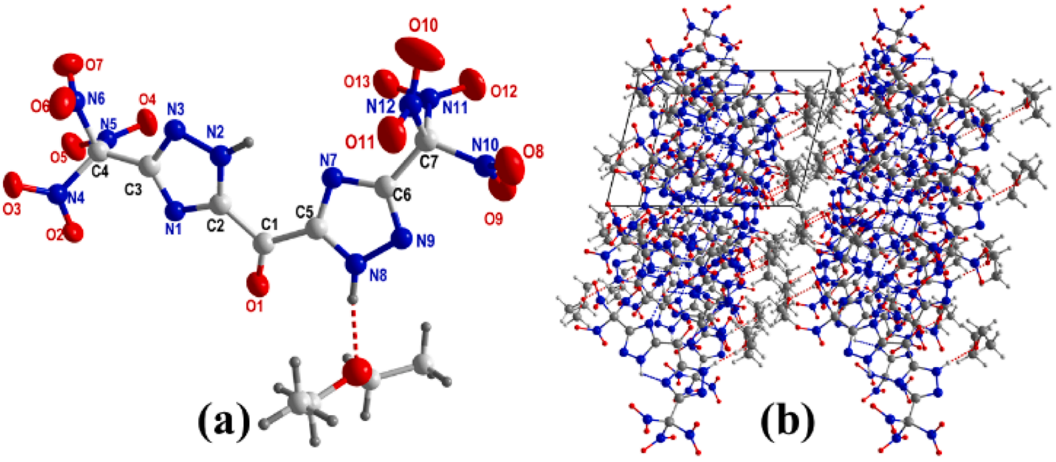

Fig. 4. (a) Molecular structure of **5**·Et_2O. (b) Packing diagram of **5**·Et_2O viewed down the b-axis. The unit cell is indicated, and dashed lines represent hydrogen bonding.

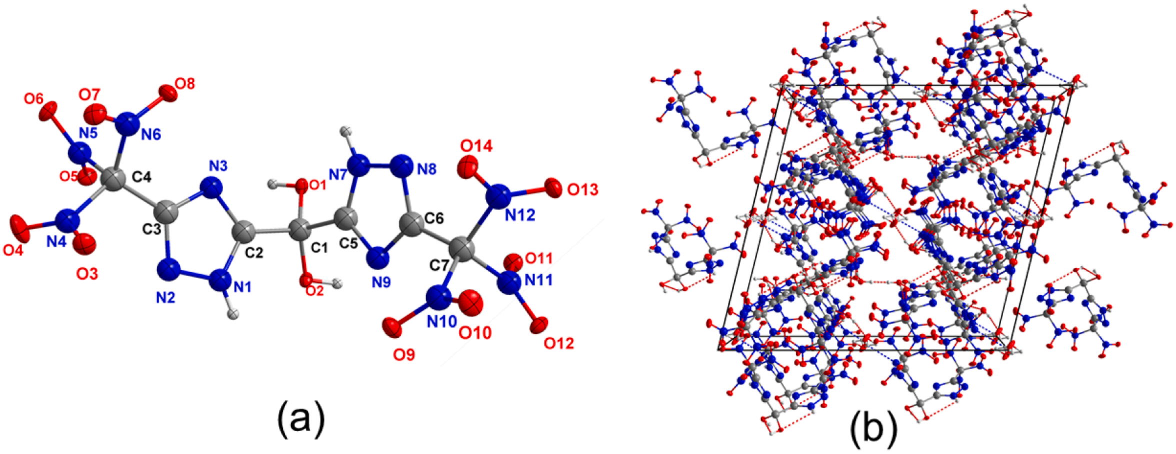

Fig. 5. (a) Molecular structure of **5a**·$3H_2O$. (b) Packing diagram of **5a**·$3H_2O$ viewed down the b-axis. Unit cell is indicated, and dashed lines represent hydrogen bonding.

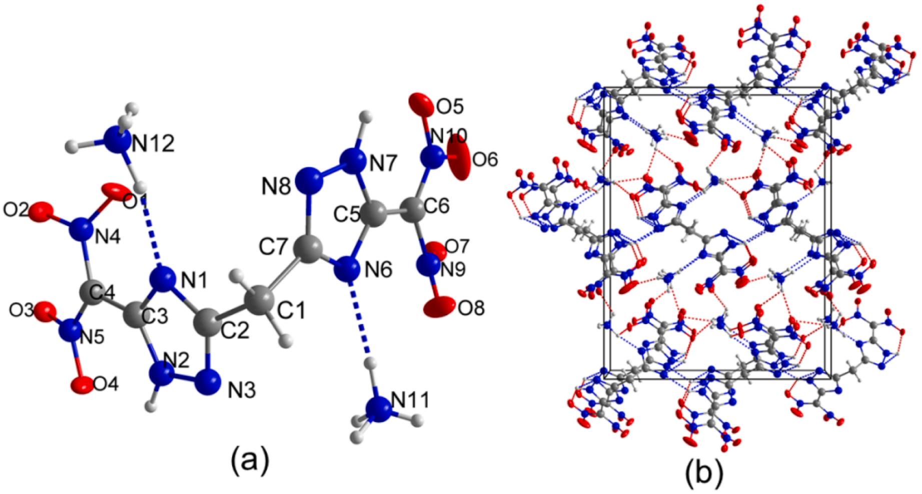

Fig. 6. (a) Molecular structure of **6**. (b) Packing diagram of **6** viewed down the b-axis. Unit cell is indicated, and dashed lines represent hydrogen bonding.

sensitivity of the *gem* diol derivative **5a**·$3H_2O$ and these properties are comparable with **5**.

2.5. Physical and detonation properties

The decomposition temperatures (onset temperature) of compounds **5**, crystals of **5a**·$3H_2O$, and **6** were measured by Differential scanning calorimetry (DSC) with a heating rate of 5 °C min^{-1}. Compound **6** has a high decomposition temperature of 183 ℃, while **5** and **5a**·$3H_2O$ have the same decomposition temperature at $T_{dec} = 150$ ℃. Both compounds **5** and **5a**·$3H_2O$ have a low decomposition temperature due to the poly nitro groups. Also, it is a clear indication that compound **5a**·$3H_2O$ has an endotherm at 80 ℃ for the loss of water molecules to regenerate the carbonyl derivative **5** (Fig. 8). Densities were measured by using a gas pycnometer at 25 ℃ where **5** is found to be 1.95 g cm^{-3}, and **5a**·$3H_2O$ at 1.82 g cm^{-3}, both of which are higher than RDX (1.80 g cm^{-3}), while **6** has a lower density of 1.75 g cm^{-3}. In addition, for comparing the experimental densities of **5** and **5a** without solvent or anhydrous molecules, we calculated the theoretical densities using the Gaussian 09 suite of programs.[27]. The theoretical density of **5** is comparable with experimental density and we believe that the results for anhydrous **5a** are more accurate (SI). Heats of formation for **5**, **5a**, **5a**·$3H_2O$, and **6** were determined by using the Gaussian 03 suite of programs.[28] For **5a**·$3H_2O$, the solid-state enthalpy of formation is calculated by adding the solid-phase heat of formation of the anhydrous compound to that of water (−241.8 kJ mol^{-1}). Compounds **5**, and **6** have high positive heats of formation, while the heats of formation of **5a**, and **5a**·$3H_2O$ are negative due to the presence of the hydroxy groups (Table 1).

For all new compounds, the detonation properties were calculated using the EXPLO5 (version 6.01) program.[29] The detonation properties of **5a**·$3H_2O$ ($P = 31.20$ GPa, $vD = 8524$ m s^{-1}) and **6** ($P = 28.91$ GPa, $vD = 8465$ m s^{-1}) are higher than **D** ($P = 28.60$ GPa, $vD = 8252$ m s^{-1}), [20] whereas **5** has higher detonation properties ($P = 39.28$ GPa, $vD = 9275$ m/s) than RDX ($P = 34.9$ GPa, $vD = 8795$ m s^{-1}) and comparable with HMX ($P = 39.2$ GPa, $vD = 9144$ m s^{-1}). Also, **5** has excellent detonation properties compared with other trinitromethyl-1,2,4-triazole derivatives, **A** ($P = 35.51$ GPa, $vD = 8983$ m s^{-1}) [17], **B** ($P = 36.20$ GPa, $vD = 9073$ m s^{-1}) [19] and **C** ($P = 36.65$ GPa, $Dv = 8964$ m s^{-1}) [17] which are already known to have better detonation properties than RDX. Compound **5** (-6.92%), with the respect to the formation of CO_2 during combustion) has a better oxygen balance compared to RDX (−22%) and HMX (−22%). The impact and friction sensitivity values were measured by using BAM Fallhammer and friction tester techniques.[30] Compound, **5** ($IS = 13$ J, $FS = 240$ N) and **5a**·$3H_2O$ ($IS = 11$ J, $FS = 240$ N) have better impact and friction sensitivites than those of compounds **C** ($IS = 1.5$ J), RDX ($IS = 7.4$ J, $FS = 120$ N) and HMX ($IS = 7.4$ J, $FS = 120$ N).

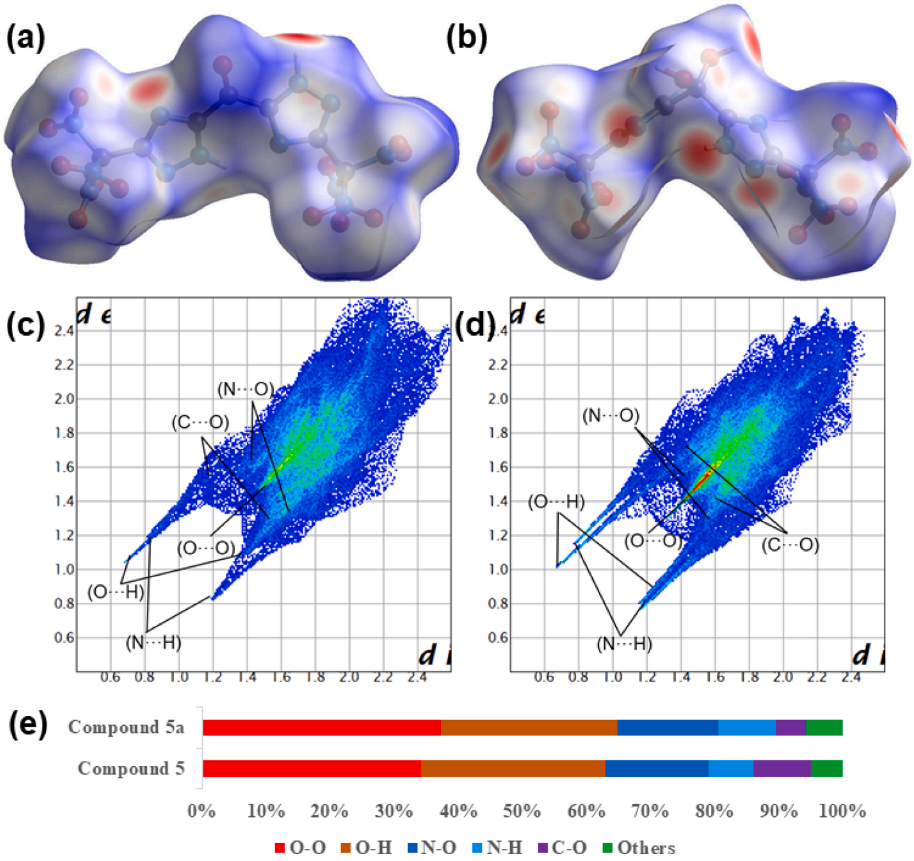

Fig. 7. Hirshfeld surface calculations and 2D fingerprint plots in the crystal structures of **5**·Et_2O and **5a**·$3H_2O$. (a) and (b) Hirshfeld surface that uses color coding to represent the proximity of close contacts around the molecules **5**·Et_2O and **5a**·$3H_2O$ (white, d = van der Waals (vdW) distance; blue, d > vdW distance; red, d < vdW distance). (c) and (d) Fingerprint plots in crystal stacking found in **5**·Et_2O and **5a**·$3H_2O$. (e) Population of close contacts in **5**·Et_2O and **5a**·$3H_2O$ in the crystal stacking. (For interpretation of the references to color in this figure legend, the reader is referred to the web version of this article.)

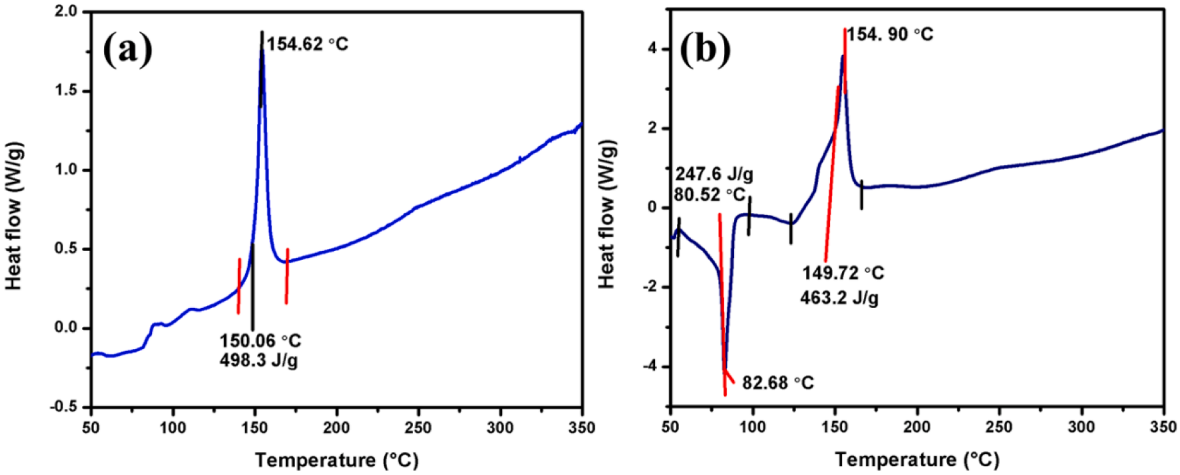

Fig. 8. DSC thermograms of Compounds **5** (a) and **5a**·$3H_2O$ (b) at the heating rate of 5 °C min^{-1}.

3. Conclusions

In summary, two simple and efficient synthetic methods were developed for the preparation of the new polynitro derivative, bis(3-(trinitromethyl)-1H-1,2,4-triazol-5-yl)methanone, **5**, in three easy and scalable synthetic steps. Compound **5** has an interesting behavior, reacting with water in organic solvents and converting to the *gem* diol, **5a**. This reactivity was not observed when the compound was isolated in water solely. The structures of carbonyl derivative **5**·Et_2O, *gem* diol derivative **5a**·$3H_2O$, and the intermediate diammonium salt **6** were confirmed by single X-ray crystallography. The measured gas pycnometer density and detonation properties of **5**, ($\rho = 1.95$ g cm^{-3}; P = 39.28 GPa, vD = 9275 m s^{-1}) were found to be superior to RDX ($\rho = 1.80$ g cm^{-3}; P = 34.90 GPa, vD = 8795 m s^{-1}) and comparable to HMX ($\rho = 1.91$ g cm^{-3}; P = 39.20 GPa, vD = 9144 m s^{-1}). In addition to this, the theoretical densities and Explo5 calculations of solvent-free molecules, **5** and **5a** suggest that expanding the functionality of carbonyl-bridged compounds may be an alternative way to achieve high-performing and less sensitive high-density materials.

4. Experimental section

Caution! All new polynitro bis-triazoles are energetic compounds with sensitivity to various stimuli. Although we have not encountered

Table 1
Properties and detonation parameters of **5**, **5a**·$3H_2O$, **6** compared with other materials.

Comp	T_{dec}[a] (°C)	ρ[b] [g cm^{-3}]	$\Delta_f H$[c] [kJ mol^{-1}/(kJ/g)]	vD[d] [m s^{-1}]	P[e] [GPa]	OB[f] (%)	O[g] (%)	I_{sp}[h] (s)	IS[i] [J]	FS[j] [N]
5	150	1.95/1.93[k]	295.5/0.63	9275	39.28	−6.92	45.0	261	13	240
5a	–	1.98[k]	−77.5/-0.16	9226	39.23	−6.70	46.65	254.4	–	–
5a·$3H_2O$	150	1.82	−802.9/-1.67	8524	31.20	−6.00	50.91	247	11	240
6	182	1.75	267.9/0.68	8465	28.91	−48.94	32.63	230	28	>360
A	124	1.94	123.2/0.46	8983	35.51	+9.12	48.7	233	9.0	–
B	133	1.89	331.9/0.76	9073	36.20	−3.69	44.2	260	22.5	252
C	133	1.83	555.1/1.20	8964	36.65	−8.60	41.5	264	1.5	–
D	164	1.94	−623.9/-1.13	8252	28.60	+8.70	49.0	219	9.0	240
RDX[l]	210	1.80	70.7/0.32	8795	34.90	−21.61	43.2	–	7.5	120
HMX[l]	280	1.91	74.8/0.25	9144	39.20	−21.61	43.2	–	7.0	120

[a] Temperature of decomposition from DSC at the heating rate of 5 °C min^{-1} (onset);
[b] Density measured by a gas pycnometer at 25 °C;
[c] Calculated molar enthalpy of formation in solid state;
[d] Calculated detonation velocity;
[e] Calculated detonation pressure;
[f] Oxygen balance based on CO_2. For a compound with the molecular formula of $C_aH_bO_cN_d$, Ω_{CO2} (%) = 1600 [(c − a − b)/Mw], Mw = molecular weight;
[g] Oxygen content;
[h] Calculated specific impulse;
[i] Impact sensitivity;
[j] Friction sensitivity;
[k] Calculated density (using hybrid density functional theory at the B3LYP/6–311++G(d,p) level of theory);
[l] Ref [15]

any difficulties or explosions in the handling of these energetic materials, all reactions should be carried out on a small scale with appropriate safety precautions (safety glasses, face shields, ear plugs, and gloves) used at all times.

5. General methods

Reagents were purchased from Oakwood Products or Beantown Chemical in analytical grade and were used as received. ^1H, and ^{13}C NMR spectra were recorded on a 300 MHz (Bruker AVANCE 300) nuclear magnetic resonance spectrometer operating at 300.13 and 75.48 MHz, respectively, by using d_6-DMSO or d_3-MeCN as the solvent and locking solvent. Tetramethyl silane and nitromethane are used as references for ^1H, ^{13}C and ^{15} NMR spectra, respectively. The ^{15}N spectra were obtained on a 500 MHz (Bruker AVANCE 500) nuclear magnetic resonance spectrometer operating at 50.69 MHz. Hirshfeld surfaces and 2D fingerprint plots for **5**·Et_2O and **5a**·$3H_2O$ were generated by CrystalExplorer 3.1.[31] The thermal decomposition points were obtained on a differential scanning calorimeter (TA Instruments Company, Model: Q2000) at a scan rate of 5 °C min^{-1}. IR spectra were recorded on a FT-IR spectrometer (Thermo Nicolet AVATAR 370) as thin films using KBr plates. Density was measured at room temperature by employing a Micromeritics AccuPyc II 1340 gas pycnometer. The impact and friction sensitivities were measured by employing a standard BAM (Bundesanstalt für Materialforschung and -Prüfung) Fallhammer and friction tester. Elemental analyses (C, H, N) were determined using a Vario Micro cube Elementar Analyser.

Single colorless needle crystals (**5**·Et_2O) of dimensions 0.16 × 0.10 × 0.06 mm^3, single colorless block crystals (**5a**·$3H_2O$) of dimensions 0.16 × 0.11 × 0.07 mm^3, and single yellow plate crystals (**6**) of dimensions 0.08 × 0.10 × 0.12 mm^3 were selected and mounted on a nylon loop with Paratone oil on a XtaLAB Synergy, Dualflex, HyPix diffractometer. The crystal was kept at a steady $T = 100(2)$ K and $T = 100.01(10)$ K during data collection, respectively. The structures were solved with the ShelXT [32] solution program using dual methods and by using Olex2 1.3-alpha and Olex2 [33] as the graphical interface. The model was refined with ShelXL 2018/3 [34] using full matrix least squares minimization on $F2$. Structure **5**·Et_2O has significant decay due and high reliability factors R1 and wR2, which were caused due to the high mobility of all the atoms in the diethyl ether molecules. In the structure of **5a**·$3H_2O$, hydrogen on the nitrogen atoms and the 2O–H groups were found and refined isotropically, the water hydrogens calculated. One water molecule is disordered over two sites via symmetry. Also, the ammonium salt **6**, shows disorder in one of the NH_4 cations and in one NO_2 group due to the poor crystallinity and lower data completion.

Diethyl 2,2′-(methylenebis(1*H*-1,2,4-triazole-5,3-diyl))diacetate (3); To a solution of malonohydrazide [35] (2.0 g, 15 mmol) in absolute ethanol (15.0 mL), ethyl 3-ethoxy-3-iminopropanoate [36] (5.3 g, 33 mmol) was added at room temperature. The resultant mixture was heated at reflux for 6 h. After cooling to room temperature, a colorless precipitate formed and was collected by filtration. It was dried in vacuo to give compound **3** (4.23 g, 86.6%). Colorless solid. T_m (5 °C min^{-1}): 172 °C (onset); ^1H NMR (300 MHz, d_6-DMSO): (ppm) 13.65 (b, s, 2H, NH), 4.12–4.05 (m, 6H, CH_2, CH_2CH_3), 3.74 (s, 2H, CH_2CO_2Et), 1.17 (t, 3H, CH_2CH_3); ^{13}C NMR (75 MHz, d_6-DMSO): (ppm) 168.8, 155.7, 154.9, 60.6, 33.4, 25.6, 13.9; IR (KBr pellet): υ 3162, 2985, 2939, 1744, 1721, 1577, 1551, 1497, 1444, 1396, 1372, 1319, 1266, 1216, 1196, 1182, 1096, 1058, 1029, 938, 873, 830, 758, 699, 671, 634, 575, 460 cm^{-1}; Elemental analysis for $C_{13}H_{18}N_6O_4$ (322.13): calcd: C, 48.44; H, 5.63; N, 26.07%. Found: C, 48.28; H, 6.42; N, 25.51%.

2,2′-(Methylenebis(1*H*-1,2,4-triazole-5,3-diyl))diacetic acid (4): Compound **3** (1.0 g, 3.10 mmol) was dissolved in aqueous sodium hydroxide (0.49 g, 12.4 mmol in 10.0 mL distilled water). The resulting mixture was stirred at 70 ℃ for 1 h. Then the reaction mixture was cooled to 0 °C and concentrated sulfuric acid added to reach pH ~ 3 followed by stirring at room temperature. A white precipitate formed, was collected by filtration, and was dried at room temperature to give pure compound **4** (0.74 g, 89%). White solid. T_m (5 °C min^{-1}): 169 °C (onset); ^1H NMR (300 MHz, d_6-DMSO): (ppm) 4.06, (s, 2H, CH_2), 3.66 (s, 4H, $2CH_2CO_2H$); ^{13}C NMR (75 MHz, d_6-DMSO): (ppm) 170.5, 156.1, 153.9, 33.5, 25.9; IR (KBr pellet): υ 3293, 3261, 2960, 2457, 1709, 1553, 1524, 1502, 1446, 1426, 1389, 1354, 1296, 1242, 1224, 1181, 1132, 1034, 942, 813, 776, 743, 707, 676, 647, 563 cm^{-1}; Elemental analysis for $C_9H_{12}N_6O_5$ (284.23): calcd: C, 38.03; H, 4.26; N, 29.57%. Found: C, 38.42; H, 4.25; N, 29.58%.

Diammonium (methylenebis(1H-1,2,4-triazole-5,3-diyl))bis (dinitromethanide) (6); A solution of concentrated sulfuric acid (6.0 mL) and fuming nitric acid (4.0 mL) was cooled to −5 ℃. Compound **3** (500 mg, 1.55 mmol) was added in small portions while maintaining the reaction temperature below 0 ℃ during addition. Then the reaction mixture was stirred at 0 ℃ for 2 h and room temperature for 10 h. The reaction was quenched by pouring into ice-cold water (~50 g). A white precipitate was formed, collected by filtration, and washed with ice-cold water (5.0 mL). The solid was dissolved in ethanol (20.0 mL) and aqueous ammonia (0.5 mL) in ethanol (2.0 mL) was added dropwise. The resulting mixture was stirred at room temperature for 2 h. A pale yellow precipitate formed, collected by filtration, and dried at room temperature to give pure compound **6** (0.52 g, 85.5%). Yellow solid. T_{dec} (5 °C min^{-1}): 182 °C (onset); ^1H NMR (300 MHz, d_6-DMSO): (ppm) 6.02 (s, 8H, $2\underline{NH_4}$), 4.09 (s, 2H, $\underline{CH_2}$); ^{13}C NMR (75 MHz, d_6-DMSO): (ppm) 156.9, 150.2, 125.5, 26.8; ^{15}N NMR (50.66 MHz, d_6-DMSO): (ppm) −22.00, −75.81, −126.72, −140.42, 360.06; IR (KBr pellet): υ 3233, 1658, 1512, 1416, 1191, 1113, 1001, 918, 825, 749, 616, 463 cm^{-1}; Elemental analysis for $C_7H_{12}N_{12}O_8$ (392.29): calcd: C, 21.43; H, 3.08; N, 42.85%. Found: C, 21.06; H, 2.59; N, 41.88%.

Bis(3-(trinitromethyl)-1H-1,2,4-triazol-5-yl)methanone (5): *Method A:* Compound **4** (1.2 g, 4.5 mmol) was dissolved in concentrated H_2SO_4 (10.0 mL) and stirred at −5 ℃ for 15 min. To this, freshly prepared fuming HNO_3 (6.0 mL) was added dropwise while maintaining the reaction temperature below 0 ℃ during addition. Then, the reaction was warmed slowly to room temperature and stirred for 24 h. The reaction mixture was poured into ice cold water (~100 g). A white precipitate formed, was collected by filtration, and washed with cold water (5.0 mL) and dried at room temperature to give pure solid compound **5** (1.75 g, 84%).

Method B: Compound **6** (0.5 g, 1.27 mmol) was dissolved in concentrated H_2SO_4 (5.0 mL) and stirred at −5 ℃ for 15 min. Freshly prepared fuming HNO_3 (2.0 mL) was added dropwise while maintaining the reaction temperature below 0 ℃ during addition. After that, the mixture was stirred for 12 h at room temperature and was poured into ice cold water (~50 g). A white precipitate formed, collected by filtration, washed with cold water (5.0 mL) and dried at room temperature giving pure compound **5** (0.43 g, 72%). White solid. T_{dec} (5 °C min^{-1}): 150 °C (onset); ^1H NMR (300 MHz, d_3-MeCN): (ppm) 13.16 (b, s, 2H, $\underline{NH}$); ^{13}C NMR (75 MHz, d_3-MeCN): (ppm) 166.8, 152.6, 150.3, 123.3; IR (KBr pellet): υ 3309, 3036, 1703, 1589, 1541, 1513, 1436, 1371, 1283, 1187, 1108, 1047, 965, 905, 844, 802, 784, 685, 646, 627, 590, 441, 416 cm^{-1}; Elemental analysis for $C_7H_2N_{12}O_{13}$ (461.98): calcd: C, 18.19; H, 0.44 N, 36.37%. Found: C, 17.76; H, 0.61; N, 36.32%.

Crystallization of compound 5a·3H_2O In a 20.0 mL glass vial, 200 mg of white solid compound **5** was dissolved in a mixed solution of acetone and distilled water (10.0 mL, in 1:1 ratio). Then the sample glass vial was placed in the open air at ambient temperature for four days. Colorless crystals were formed and were collected by filtration and dried at room temperature to give compound **5a**·3H_2O (0.19 g, 82%). Colorless crystals. T_m (5 °C min^{-1}): 82 °C (onset); T_{dec} (5 °C min^{-1}): 150 °C (onset); ^1H NMR (300 MHz, d_6-DMSO): (ppm) 4.88 (b, s, 4H, $2\underline{NH}$, $2\underline{OH}$); ^{13}C NMR (75 MHz, d_6-DMSO): (ppm) 160.8, 148.3, 123.3, 88.7; ^{15}N NMR (50.66 MHz, d_6-DMSO): (ppm) −32.33, −75.01, −126.15, −157.01; IR (KBr pellet): υ 3307, 3034, 1703, 1604, 1437, 1371, 1285, 1204, 1108, 1048, 966, 906, 844, 801, 750, 687, 646 cm^{-1}; Elemental analysis for $C_7H_{10}N_{12}O_{17}$ (534.02): calcd: C, 15.74; H, 1.89 N, 31.46%. Found: C, 16.11; H, 1.88; N, 31.99%.

Declaration of Competing Interest

The authors declare that they have no known competing financial interests or personal relationships that could have appeared to influence the work reported in this paper.

Acknowledgement

The Rigaku Synergy S Diffractometer was purchased with support from the National Science Foundation MRI program under Grant No. 1919565.

Appendix A. Supplementary data

Supplementary data to this article can be found online at https://doi.org/10.1016/j.cej.2021.133520.

References

[1] T.M. Klapötke, Chemistry of High-energy Materials, De Gruyter, Berlin (2011), https://doi.org/10.1515/9783110624571.

[2] D. Fischer, J.L. Gottfried, T.M. Klapötke, K. Karaghiosoff, J. Stierstorfer, T. G. Witkowski, Synthesis and investigation of advanced energetic materials based on bispyrazolylmethanes, Angew. Chem. Int. Ed. 128 (52) (2016) 16366–16369, https://doi.org/10.1002/ange.201609267.

[3] J. P. Agrawal, High energy materials: propellants, explosives and pyrotechnics; Wiley-Vch Verlag GmbH & Co. KGaA, Weinheim, 2010. Doi: 10.1002/9783527628803.

[4] O. Bolton, A.J. Matzger, Improved stability and smart-material functionality realized in an energetic cocrystal, Angew. Chem. Int. Ed. 50 (38) (2011) 8960–8963, https://doi.org/10.1002/anie.v50.3810.1002/anie.201104164.

[5] H. Gao, J.M. Shreeve, Azole-based energetic salts, Chem. Rev. 111 (11) (2011) 7377–7436, https://doi.org/10.1021/cr200039c.

[6] Z. Dong, Z. Ye, Synthesis and properties of salts derived from $C_4N_{18}^{2-}$, $C_4N_{18}H^{3-}$ and $C_4N_{18}H_3^-$ anions, J. Mater. Chem. A 8 (47) (2020) 25035–25039, https://doi.org/10.1039/D0TA08153A.

[7] Y. Zhou, H. Gao, J.M. Shreeve, Dinitromethyl groups enliven energetic salts, Energy Mater. Front. 1 (1) (2020) 2–15, https://doi.org/10.1016/j.enmf.2020.04.001.

[8] J. Zhang, S. Dharavath, L.A. Mitchell, D.A. Parrish, J.M. Shreeve, Energetic salts based on 3,5-bis(dinitromethyl)-1,2,4-triazole monoanion and dianion: Controllable preparation, characterization, and high performance, J. Am. Chem. Soc. 138 (24) (2016) 7500–7503, https://doi.org/10.1021/jacs.6b0381910.1021/jacs.6b03819.s00110.1021/jacs.6b03819.s00210.1021/jacs.6b03819.s00310.1021/jacs.6b03819.s004.

[9] P. Yin, J. Zhang, L.A. Mitchell, D.A. Parrish, J.M. Shreeve, 3,6-Dinitropyrazolo[4,3-c]pyrazole-based multipurpose energetic materials through versatile-functionalization strategies, Angew. Chem. Int. Ed. 55 (2016) 12895–12897, https://doi.org/10.1002/anie.201606894.

[10] Q. Yu, P. Yin, J. Zhang, C. He, G.H. Imler, D.A. Parrish, J.M. Shreeve, Pushing the limits of oxygen balance in 1,3,4-oxadiazoles, J. Am. Chem. Soc. 139 (26) (2017) 8816–8819, https://doi.org/10.1021/jacs.7b0515810.1021/jacs.7b05158.s00110.1021/jacs.7b05158.s00210.1021/jacs.7b05158.s00310.1021/jacs.7b05158.s00410.1021/jacs.7b05158.s00510.1021/jacs.7b05158.s007.

[11] G. Zhao, D. Kumar, P. Yin, C. He, G.H. Imler, D.A. Parrish, J.M. Shreeve, Construction of polynitro compounds as high performance oxidizers via a two-step nitration of various functional groups, Org. Lett. 21 (4) (2019) 1073–1077, https://doi.org/10.1021/acs.orglett.8b0411410.1021/acs.orglett.8b04114.s001.

[12] Q. Yu, G.H. Imler, D.A. Parrish, J.M. Shreeve, Challenging the limits of nitro groups associated with a tetrazole ring, Org. Lett. 21 (12) (2019) 4684–4688, https://doi.org/10.1021/acs.orglett.9b0156510.1021/acs.orglett.9b01565.s001.

[13] R. Haiges, G. Bélanger-Chabot, S.M. Kaplan, K.O. Christe, Preparation and characterization of 3,5-dinitro-1h-1,2,4-triazole, Dalton Trans. 44 (16) (2015) 7586–7594, https://doi.org/10.1039/C5DT00888C.

[14] A.A. Dippold, T.M. Klapötke, Nitrogen-rich bis-1,2,4-triazoles-a comparative study of structural and energetic properties, Chem.−Eur. J. 18 (52) (2012) 16742–16753, https://doi.org/10.1002/chem.v18.5210.1002/chem.201202483.

[15] H. Gao, Q. Zhang, J.M. Shreeve, Fused heterocycle-based energetic materials (2012–2019), J. Mater. Chem. A 8 (8) (2020) 4193–4216, https://doi.org/10.1039/C9TA12704F.

[16] S. Dharavath, J. Zhang, G.H. Imler, D. Parrish, J.M. Shreeve, 5-(Dinitromethyl)-3-(trinitromethyl)-1,2,4-triazole and its derivatives: a new application of oxidative nitration towards gem-trinitro-based energetic material, J. Mater. Chem. A 5 (2017) 4785–4790, https://doi.org/10.1039/C7TA00730B.

[17] V. Thottempudi, H. Gao, J.M. Shreeve, Trinitromethyl-substituted 5-nitro-or 3-azo-1, 2, 4-triazoles: synthesis, characterization, and energetic properties, J. Am. Chem. Soc. 133 (16) (2011) 6464–6471, https://doi.org/10.1021/ja2013455.

[18] M. A. Petrie, G. Koolpe, R. Malhotra, P. Penwell, ONR final report, SRI international, SRI Project No. PI8608, March 2012.

[19] Q. Ma, H. Gu, J. Huang, F. Nie, G. Fan, L. Liao, W. Yang, Formation of trinitromethyl functionalized 1,2,4-triazole-based energetic ionic salts and a zwitterionic salt directed by an intermolecular and intramolecular metathesis strategy, New J. Chem. 42 (4) (2018) 2376–2380, https://doi.org/10.1039/C7NJ03939E.

[20] G. Zhao, P. Yin, D. Kumar, G.H. Imler, D.A. Parrish, J.M. Shreeve, Bis(3-nitro-1-(trinitromethyl)-1H-1,2,3-triazol-5-yl)- methanone: An applicable and very dense green oxidizer, J. Am. Chem. Soc. 141 (2019) 19581–19584, https://doi.org/10.1021/jacs.9b11326.

[21] W.J. Middleton, R.V. Lindsey, Hydrogen bonding in fluoro alcohols, J. Am. Chem. Soc. 86 (22) (1964) 4948–4952, https://doi.org/10.1021/ja01076a041.

[22] M. Freis, T.M. Klapötke, J. Stierstorfer, N. Szimhardt, Di(1H-tetrazol-5-yl)methane as neutral ligand in energetic transition metal complexes, Inorg. Chem. 56 (14) (2017) 7936–7947, https://doi.org/10.1021/acs.inorgchem.7b0043210.1021/acs.inorgchem.7b00432.s001.

[23] Z. Bo, C. Sitong, G. Weiming, Z. Weijing, W. Lin, Y. Li, Z. Jianguo, Gem-diol and ketone crystal-to-crystal transition phenomena, Sci. Rep. 7 (2017) 13426, https://doi.org/10.1038/s41598-017-13596-6.

[24] A.M.M. Rawashdeh, A. Thangavel, C. Sotiriou-Leventis, N. Leventis, Control of the ketone to gem-diol equilibrium by host−guest interactions, Org. Lett. 10 (6) (2008) 1131–1134, https://doi.org/10.1021/ol800021r10.1021/ol800021r.s002.

[25] M.A. Spackman, J.J. McKinnon, Fingerprinting intermolecular interactions in molecular crystals, CrystEngComm 4 (66) (2002) 378–392, https://doi.org/10.1039/B203191B.

[26] M.A. Spackman, D. Jayatilaka, Hirshfeld surface analysis, CrystEngComm 11 (1) (2009) 19–32, https://doi.org/10.1039/B818330A.

[27] Gaussian 09(Revision E.01), M. J. Frisch, G. W. Trucks, H. B. Schlegel, G. E. Scuseria, M. A. Robb, J. R. Cheeseman, G. Scalmani, V. Barone, B. Mennucci, G. A. Petersson, H. Nakatsuji, M. Caricato, X. Li, H. P. Hratchian, A. F. Izmaylov, J. Bloino, G. Zheng, J. L. Sonnenberg, M. Hada, M. Ehara, K. Toyota, R. Fukuda, J. Hasegawa, M. Ishida, T. Nakajima, Y. Honda, O. Kitao, H. Nakai, T. Vreven, J. A. Montgomery Jr., J. E. Peralta, F. Ogliaro, M. Bearpark, J. J. Heyd, E. Brothers, K. N. Kudin, V. N. Staroverov, T. Keith, R. Kobayashi, J. Normand, K. Raghavachari, A. Rendell, J. C. Burant, S. S. Iyengar, J. Tomasi, M. Cossi, N. Rega, J. M. Millam, M. Klene, J. E. Knox, J. B. Cross, V. Bakken, C. Adamo, J. Jaramillo, R. Gomperts, R. E. Stratmann, O. Yazyev, A. J. Austin, R. Cammi, C. Pomelli, J. W. Ochterski, R. L. Martin, K. Morokuma, V. G. Zakrzewski, G. A. Voth, P. Salvador, J. J. Dannenberg, S. Dapprich, A. D. Daniels, O. Farkas, J. B. Foresman, J. V. Ortiz, J. Cioslowski and D. J. Fox, Gaussian, Inc., Wallingford CT, 2013.

[28] Gaussian 03(Revision E.01), M. J. Frisch, G. W. Trucks, H. B. Schlegel, G. E. Scuseria, M. A. Robb, J. R. Cheeseman, J. A. Montgomery, Jr., T. Vreven, K. N. Kudin, J. C. Burant, J. M.Millam, S. S. Iyengar, J. Tomasi, V. Barone, B. Mennucci, M. Cossi, G. Scalmani, N. Rega, G. A. Petersson, H. Nakatsuji, M. Hada, M. Ehara, K. Toyota, R. Fukuda, J. Hasegawa, M. Ishida, T. Nakajima, Y. Honda, O. Kitao, H. Nakai, M. Klene, X. Li, J. E. Knox, H. P. Hratchian, J. B. Cross, V. Bakken, C. Adamo, J. Jaramillo, R. Gomperts, R. E. Stratmann, O. Yazyev, A. J. Austin, R. Cammi, C. Pomelli, J. W. Ochterski, P. Y. Ayala, K. Morokuma, G. A. Voth, P. Salvador, J. J. Dannenberg, V. G. Zakrzewski, S. Dapprich, A. D. Daniels, M. C. Strain, O. Farkas, D. K. Malick, A. D. Rabuck, K. Raghavachari, J. B. Foresman, J. V. Ortiz, Q. Cui, A. G. Baboul, S. Clifford, J. Cioslowski, B. B. Stefanov, G. Liu, A. Liashenko, P. Piskorz, I. Komaromi, R. L.Martin, D. J. Fox, T. Keith, M. A. Al-Laham, C. Y. Peng, A. Nanayakkara, M. Challacombe, P. M. W. Gill, B. Johnson, W. Chen, M. W. Wong, C. Gonzalez and J. A. Pople,Gaussian, Inc.,Wallingford CT, 2004.

[29] EXPLO5, version 6.01, M. Sućeska, 2013.

[30] (a) A 20 mg sample was subjected to a drop-hammer test with a 5 or 10 kg dropping weight. The impact sensitivity was characterized according to the UN recommendations (insensitive, >40 J; less sensitive, 35 J; sensitive, 4 J; very sensitive, 3 J); (b) United Nations, Recommendations on the transport of dangerous goods, manual of tests and criteria, New York, 5th Rev. Edn, 2009.

[31] S. K. Wolff, D. J. Grimwood, J. J. McKinnon, M. J. Turner, D. Jayatilaka, M. A. Spackman CrystalExplorer (Version 3.1), University of Western Australia, 2012.

[32] G.M. Sheldrick, Crystal structure refinement with SHELXL, Acta Cryst. A71 (2015) 3–8, https://doi.org/10.1107/S2053229614024218.

[33] O.V. Dolomanov, L.J. Bourhis, R.J. Gildea, J.A.K. Howard, H. Puschmann, OLEX2: a complete structure solution, refinement and analysis program, J. Appl. Cryst. 42 (2) (2009) 339–341, https://doi.org/10.1107/S0021889808042726.

[34] G.M. Sheldrick, Crystal structure refinement with SHELXL, Acta Cryst. C71 (2015) 3–8, https://doi.org/10.1107/S2053229614024218.

[35] R. Arunachalam, C.S. Aswathi, A. Das, R.I. Kureshy, P.S. Subramanian, Diastereoselective nitroaldol reaction catalyzed by binuclear copper (ii) complexes in aqueous medium, ChemPlusChem 80 (1) (2015) 209–216, https://doi.org/10.1002/cplu.v80.110.1002/cplu.201402200.

[36] M.S. Mishina, A.Y. Ivanov, P.S. Lobanov, D.V. Dar'in, A new synthesis of 2-aminoindoles and 6-aminopyrrolo[3,2-d]pyrimidines from π-deficient 1,2-dihaloarenes and geminal enediamines, Synthesis 48 (2016) 2851–2862, https://doi.org/10.1055/s-0035-1561645.